ACS APPLIED MATERIALS & INTERFACES

Research Article

www.acsami.org

Charged Micropollutant Removal With Hollow Fiber Nanofiltration Membranes Based On Polycation/Polyzwitterion/Polyanion Multilayers

Joris de Grooth, Dennis M. Reurink, Jeroen Ploegmakers, Wiebe M. de Vos,* and Kitty Nijmeijer

Membrane Science and Technology, MESA+ Institute for Nanotechnology, University of Twente, P.O. Box 217, 7500 AE Enschede, The Netherlands

ABSTRACT: Hollow fiber nanofiltration membranes can withstand much higher foulant concentrations than their spiral wound counterparts and can be used in water purification without pretreatment. Still, the preparation of hollow fiber nanofiltration membranes is much less established. In this work, we demonstrate the design of a hollow fiber nanofiltration membrane with excellent rejection properties by alternatively coating a porous ultrafiltration membrane with a polycation, a polyzwitterion, and a polyanion. On model surfaces, we show, for the first time, that the polyzwitterion poly *N*-(3-sulfopropyl)-*N*-(methacryloxyethyl)-*N*,*N*-dimethylammonium betaine (PSBMA) can be incorporated into traditional polyelectrolyte multilayers based on poly(styrenesulfonate) (PSS) and poly(diallyldimethylammonium chloride) (PDADMAC). Furthermore, work on model surfaces allows a good characterization of, and insight into, the layer build-up and helps to establish the optimal membrane coating conditions. Membranes coated with these multilayers have high salt rejection of up to 42% NaCl, 72% $CaCl_2$, and 98% Na_2SO_4 with permeabilities of 3.7−4.5 $l{\cdot}m^{-2}{\cdot}h^{-1}{\cdot}bar^{-1}$. In addition to the salt rejections, the rejection of six distinctively different micropollutants, with molecular weights between 215 and 362 $g{\cdot}mol^{-1}$, was investigated. Depending on the terminating layer, the incorporation of the polyzwitterion in the multilayer results in nanofiltration membranes that show excellent retentions for both positively and negatively charged micropollutants, a behavior that is attributed to dielectric exclusion of the solutes. Our approach of combining model surfaces with membrane performance measurements provides unique insights into the properties of polyzwitterion-containing multilayers and their applications.

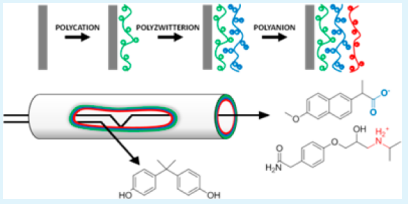

KEYWORDS: *polyelectrolyte multilayer, nanofiltration, polyzwitterion, hollow fiber membrane modification, micropollutants*

1. INTRODUCTION

The intensification of the use and reuse of freshwater resources comes at a cost. Reports on rising levels of emerging contaminants in our water are numerous.[1−4] And with the world population growing in number, age, and level of welfare, the strain that these newborn contaminants puts on drinking water will only increase. After the successful development of treatment methods based on porous membranes (e.g., ultrafiltration (UF)) that are designed to remove harmful yet mainly macroscopic sized contaminants such as bacteria, cryptosporidium, and viruses, the development of the next generation membranes for water treatment is essential. The main focus will lie on the removal of small organic contaminants that are typically harmful after prolonged exposure to low concentrations.[3] These emerging contaminants, also called micropolutants (MPs), are industrial, medicinal, and agricultural wastes such as nonylphenols, sulfamethoxazole, atenolol, and atrazine.[3,5] They are characteristically small, with molecular weights (M_r) ranging between 100 and 1000 Da, and have the potential to cause long-term harm to humans and the environment. Because of their small size, conventional membrane filtration with relatively large pores, such as UF and microfiltration (MF), is not sufficient for their removal.

Using nanofiltration (NF) membranes has been proposed as a cost-effective method to remove micropollutants.[6] Numerous studies have shown that commercially available NF membranes are capable of retaining several contaminants, but the rejection depends on the properties of the micropollutant.[7−15] Although the rejections of NF membranes are significantly lower compared to those of reverse osmosis (RO), it is argued that this drawback can be overcome by an appropriate post-treatment.[6] All commercially available NF membranes (e.g., NF270 and NF90 from DOW, ESNA from Hydranautics, and TFC-SR3 from Koch) are flat sheet membranes in a spiral wound module, which have limited hydraulic and chemical cleaning possibilities. This means that in addition to the optional post-treatment, an extensive pretreatment (e.g., UF or rapid sand filtration) of the feed is required in order to reduce (bio)fouling on the spacers and the membrane.[16,17] The pretreatment comes with additional operational costs,[18] and a significant cost saving can thus be obtained if this pretreatment could be skipped by using hollow fiber NF membranes instead of spiral wound NF membranes (Figure 1).[19] Just as is the case for hollow fiber UF membranes, hollow fiber NF membranes

Received: July 15, 2014
Accepted: September 9, 2014
Published: September 9, 2014

dx.doi.org/10.1021/am504630a | *ACS Appl. Mater. Interfaces* 2014, 6, 17009−17017

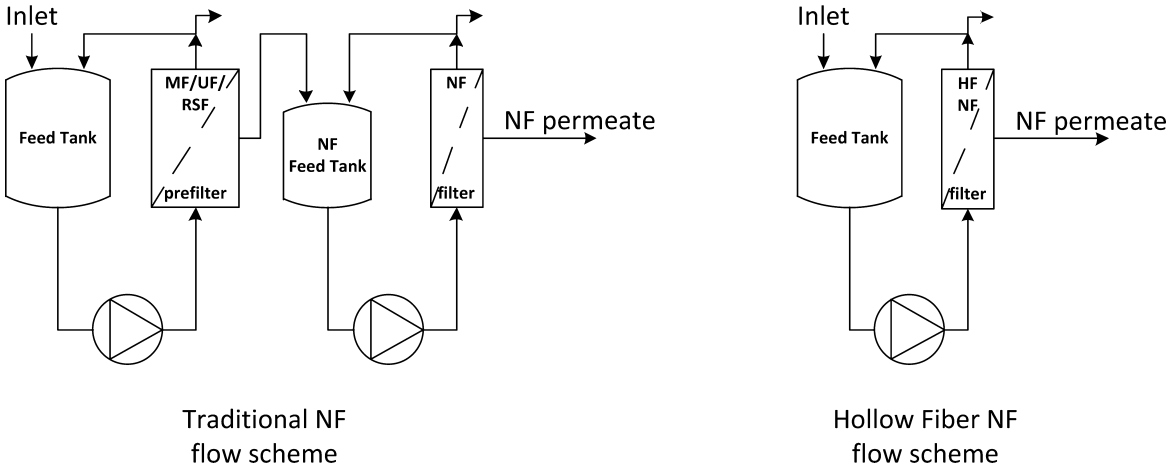

Figure 1. Flow scheme of (left) a traditional spiral wound NF process with an additional pretreatment for the feed and (right) of the proposed direct hollow fiber NF process without pretreatment.

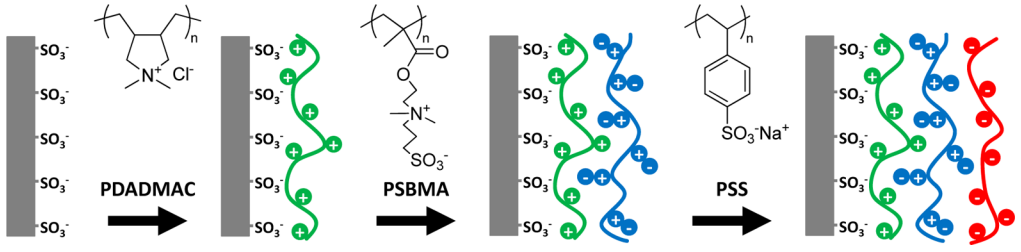

Figure 2. Schematic representation of the coating of a charged hollow fiber membrane with a trilayer of PDADMAC (+), PSBMA (z), and PSS (−) on a charged hollow fiber membrane.

are able to withstand much higher foulant concentrations without any detrimental effects such as spacer clogging. Unfortunately, commercial hollow fiber NF membranes for these applications are scarce, with the only choice at the moment being Pentair X-Flow's HFW 1000 membrane, which has a relatively high molecular weight cutoff of approximately 1000 Da. This means that there is a strong need for the development of hollow fiber membranes with dense NF filtration properties.

Several methods have been investigated to obtain hollow fiber membranes with NF-like properties. Thin polyamide layers have been applied on hollow fibers via interfacial polymerization, an approach very similar to that of the thin film composite (TFC) spiral wound membranes.[20] However, these TFC composite polyamide layers are easily degraded in the presence of oxidizing agents. This significantly limits the possibilities to remove (bio)fouling from the membrane (e.g., via oxidation with hypochlorite), as this would harm the performance of the membrane over time.[21] Additionally, due to of the lack of pretreatment, the hollow fiber NF feed will have a much higher foulant load that will require a NF layer designed to cope with this. We therefore argue that successful hollow fiber NF membranes should either be stable against hypochlorite degradation or have good antifouling properties. For chemically stable NF membranes, dense layers of sulfonated poly(ether ether ketone) (SPEEK) are coated, typically on top of poly(ether sulfone) (PES) supports.[22] Jung et al. applied a thin layer of SPEEK on hollow fiber UF membranes to remove aromatic pesticides,[23] while in a comparable way, SPEEK was used by Song et al. to remove glyphosate.[24] Recently, a more facile method for membrane modification based on the self-assembly of oppositely charged polyelectrolytes has received increased attention.[25−27] In this so-called layer-by-layer (LbL) assembly, a substrate is alternatively exposed to polycations and polyanions to build polyelectrolyte multilayers (PEMs) of controllable thickness.[28] The versatility of this approach allows the PEMs to be grown on a multitude of substrates, thus enabling its use for the development of hollow fiber NF.[29,30] By choosing chemically stable polyelectrolytes, dense thin layers that have increased chemical cleaning possibilities or low fouling resistance can be obtained. In addition to polycations and polyanions, other (multi)functional macromolecules can be incorporated into the multilayer, leading to enhanced properties of the layers.[31−34] An example of these macromolecules are polyzwitterions, polymers that contain both positive and negative moieties on the same monomer. Polyzwitterions exhibit unique properties, such as low-fouling coatings, sensors, and chromatography, which make them interesting materials for a variety of applications.[35,36] Moreover, NF membranes with grafted zwitterionic moieties have been shown to have improved rejections and improved antifouling properties.[37,38] For LbL systems, it was shown by Kharlampieva et al. that under acidic conditions, weak polyzwitterions can be incorporated into traditional multilayers.[31] In a previous study, we showed that the site-specific interactions between a strong polyzwitterion and a polycation can also be used to grow zwitterionic multilayers for stimuli responsive membranes without the need for acidic conditions.[39]

In this work, we employ the LbL concept using zwitterionic polymers for the development of the next generation hollow fiber NF membranes and show that the retention behavior of these membranes for emerging contaminants can be tailored, depending on the intrinsic properties of the applied layers. We

report, for the first time, on the incorporation of the polyzwitterion poly *N*-(3-sulfopropyl)-*N*-(methacryloxyethyl)-*N*,*N*-dimethylammonium betaine (PSBMA) in LbL assembled multilayers of poly(diallyldimethylammonium chloride) (PDADMAC), a strong polycation, and poly(styrenesulfonate) (PSS), a strong polyanion. Trilayers of PDADMAC/PSBMA/PSS are formed. The effect of ionic strength on the trilayer assembly on silicon wafers as model surfaces is investigated to understand the layer growth. Similar layers are then coated on charged polymeric membranes to make hollow fiber NF membranes (Figure 2), which are characterized by means of water permeability and ion and micropollutant rejection. Finally, the fundamental insights of the layer growth obtained from model surfaces are correlated to the permeability and rejection behavior of the developed hollow fiber NF membranes.

2. EXPERIMENTAL SECTION

2.1. Materials. An aqueous solution of 20 wt % polydiallyldimethylammonium chloride (PDADMAC, M_r = 150 kDa) was obtained from Kemira (Finland). An aqueous solution of 20 wt % polystyrene sulfonic acid (PSS, M_r = 100 kDa) was obtained from Tosoh Organic Chemical Co., LTD (Japan). *N*-(3-Sulfopropyl)-*N*-(methacryloxyethyl)-*N*,*N*-dimethylammonium betaine (SBMA) was obtained from Sigma-Aldrich (The Netherlands) and used for polymerization without any further purification steps. The PSBMA was synthesized via an aqueous radical polymerization of SBMA with sodium peroxidisulfate at 70 °C and has a molecular weight of 500 kDa. The PSBMA synthesis and characterization is described in more detail elsewhere.[39] All other chemicals were purchased from Sigma-Aldrich (The Netherlands).

2.2. Reflectometry. The multilayer growth on silicon wafers was monitored by means of reflectometry.[40] For this, 0.1 g·l^{-1} cationic, zwitterionic, and anionic polymer solutions with the appropriate ionic strength were prepared and alternatively adsorbed onto a silicon wafer with a 75 nm SiO_2 top layer. The use of a stagnation point flow cell allows for very well-controlled hydrodynamics during the multilayer growth. Polarized monochromatic light (He−Ne laser, 632.8 nm) hits the wafer around the Brewster angle and is reflected toward the detector. The reflected light is split into its p- and s- polarized components. The ratio between these two components is defined as S (−), and the change in this ratio (ΔS) is directly proportional to the amount of mass adsorbed on the wafer, according to eq 1:

$$\Gamma = \frac{\Delta S}{S_0} Q \tag{1}$$

where Γ is the amount of mass adsorbed on the wafer (mg·m^{-2}), S_0 is the starting output signal of the bare silicon wafer (−), and Q is the sensitivity factor for the system (mg·m^{-2}). To calculate the sensitivity factor, we used an optical model based on the following values: θ = 71°, n_{silica} = 1.46, $\tilde{n}_{silicon}$ = (3.85, 0.02), n_{H_2O} = 1.33, $dn/dc_{PDADMAC}$ = 0.18 mL·g^{-1}, dn/dc_{PSBMA} = 0.14 mL·g^{-1}, dn/dc_{PSS} = 0.18 mL·g^{-1}, d_{silica} = 75 nm.[39,41] The sensitivity factor (Q) obtained to calculate the actual mass adsorption for all experiments is 30 mg·m^{-2}, a value that was validated by atomic force microscopy measurements for similar layers in our previous work.[39]

2.3. Contact Angle. Optical contact angle measurements were performed on an OCA15 plus from Dataphysics Instruments. For this, silicon wafers were dip-coated for 20 min in 0.1 g·l^{-1} cationic, zwitterionic, or anionic polymer solutions with 0.2 M NaCl in an alternating fashion. After each single polymer addition, the coated wafers were rinsed with a background electrolyte solution of 0.2 M NaCl for 20 min. The contact angle of the sessile drop of 2 μL of water on the appropriate LbL coating was measured five times for each coating at 22 °C, and the average and standard deviation are reported. The contact angles were measured 5 s after the bubble was placed on the surface.

2.4. Membrane Modification and Characterization. Polyelectrolyte multilayers were coated on dense ultrafiltration membranes prepared from sulfonated poly(ether sulfone) (hollow fiber silica (HFS), kindly provided by Pentair X-Flow (The Netherlands). These are hollow fiber membranes with a molecular weight cutoff of 10 kDa.

Before the coating of the membranes, we first wetted the fibers overnight in a 15 wt % ethanol solution in water and rinsed them with demineralized water. The membranes were coated via a simple dip-coating procedure. For the trilayer coatings, the fibers were completely immersed in a 0.1 g·l^{-1} polycation solution with 0.2 M NaCl at room temperature. After 30 min, the fibers were subsequently rinsed in three separate solutions containing only NaCl with an ionic strength similar to that of the coating solution for 10 min in each solution, after which a membrane sample was taken. The remaining samples were subsequently dipped for 30 min in an alternating fashion in PSBMA, PSS, and PDADMAC solutions with 0.2 M NaCl, taking a membrane sample after each coating step. After being rinsed, all membrane samples were put in a glycerol/water (15/85 wt %) mixture for 4 h and dried overnight under ambient conditions. For the filtration experiments, single PEM-coated membrane fibers were potted in a module with a fiber length of approximately 200 mm.

The water permeability (l·m^{-2}·h^{-1}·bar^{-1}) was calculated by normalizing the measured pure water flux with the trans membrane pressure. The pure water flux was measured at 20 °C with demineralized water in dead-end mode at a trans-membrane pressure of 2 bar. The membrane permeability was measured for two separate coating experiments, each in duplicate. The average of the permeability and the standard deviation is reported. For the salt retention measurements, a cross-flow through the fibers was applied. To limit the effect of concentration polarization, we set the cross-flow velocity of the feed through the fibers at 4.6 m·s^{-1}. This corresponds to a Reynolds number of approximately 3500, well above the transition to turbulent flow. The salt concentrations of the retentate and permeate were measured with a WTW Cond 3210 conductivity meter. The retention was based on the ratio between the permeate and concentrate concentrations.

The zeta potential of the membranes was determined with a SurPASS electrokinetic analyzer (Anton Paar, Graz, Austria). The zeta potential was calculated by measuring the streaming current versus the pressure in a 5 mM KCl solution (pH 5.8) at room temperature, using the following equation:

$$\zeta = \frac{dI}{dP}\frac{\eta}{\varepsilon\varepsilon_0}\kappa_B R \tag{2}$$

where ζ is de zeta potential (V), I is the streaming current (A), P is the pressure (Pa), η is the dynamic viscosity of the electrolyte solution (Pa·s), ε is the dielectric constant of the electrolyte (−), ε_0 is the vacuum permittivity (F·m^{-1}), κ_B is the bulk electrolyte conductivity (S·m^{-1}), and R is the electrical resistance (Ω) inside the streaming channel. For each point, the zeta potential is measured four times for two different membranes, and the average and standard deviation is reported.

2.5. Micropollutant Analysis. For the characterization of the NF membranes, a selection of six common micropollutants (Figure 3) has been made for rejection experiments. The micropollutant molecular weight range is between 200 and 400 g·mol^{-1}, in the order of the typical molecular weight cutoff (MWCO) of NF membranes. The selection is made such that it covers neutral, positive, and negative molecules at the measurement pH of 5.8 and contains both hydrophobic and hydrophilic molecules (Table 1). This ensures that the role of the solute charge can be properly assessed. Solutions containing all six micropollutants at a concentration of 10 mg·l^{-1} each were filtered through the prepared membranes for at least 24 h before collecting the permeate sample. This filtration time is needed to ensure steady state rejections. To reduce concentration polarization, we applied a cross-flow velocity of around 4.6 m·s^{-1}. The trans-membrane pressure during filtration was 1.75 bar. Micropollutant rejections were calculated based on the differences between permeate and concentrate concentrations. The micropollutant concentrations in the feed and

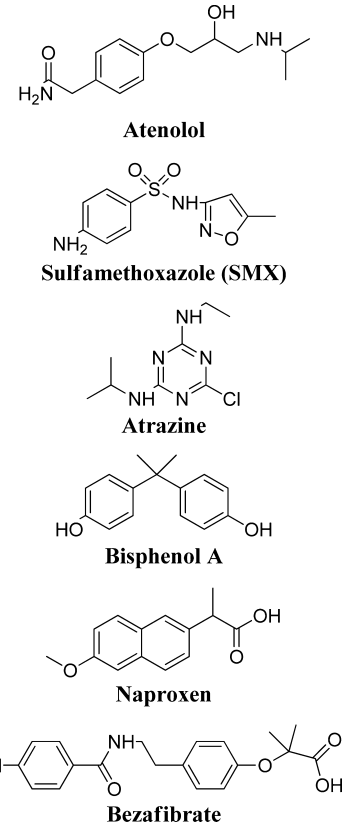

Figure 3. Chemical structures of the six micropollutants selected for this work.

Table 1. Properties of the Six Micropollutants Selected for This Work[a]

	pK_a	log P	M_r (g·mol^{-1})	charge (pH 5.8)
atenolol	9.7	0.43	266.33	+
SMX	2.0/7.7	0.79	253.28	0
atrazine	3.2	2.20	215.68	0
bisphenol A	10.1	4.04	228.29	0
naproxen	4.2	2.99	230.26	−
bezafibrate	3.8	3.99	361.819	−

[a]Chemicalize.org by ChemAxon was used for generating the structure property prediction (http://www.chemicalize.org).

permeate were determined via liquid chromatography. For this, a Dionex Ultimate 3000 U-HPLC system equipped with an RS variable wavelength detector was used. Micropollutant separation was done on an Acclaim RSLC C18 2.2 μm column (Thermo Scientific) at 65 °C, while applying a gradient flow from 95 wt % H_2O + 5 wt % acetonitrile at pH 4 to 5 wt % H_2O + 95 wt % acetonitrile at 1 mL·min^{-1}.

3. RESULTS AND DISCUSSION

3.1. Multilayer Growth. The multilayer growth on silicon wafers is monitored in situ with reflectometry. A silicon wafer is exposed to 0.1 g·l^{-1} solutions of PDADMAC (+), PSBMA (z) and PSS (−) until a stable plateau in the adsorbance is obtained. All solutions contain a background electrolyte, and the different polyelectrolytes are coated in an alternating fashion, as shown in Figure 4. Before switching to a different polyelectrolyte solution, the measurement cell is always rinsed with the appropriate background electrolyte solutions for at least 100 s to prevent any possible bulk association of polyelectrolytes. The results of the multilayer growth at different ionic strengths is shown in Figure 4, where the polyelectrolyte adsorption (mg·m^{-2}) is plotted as a function of time.

Figure 4 clearly shows, for the first time, the possibility of the formation of PDADMAC/PSBMA/PSS trilayers on a silicon wafer. The results also show a significant dependence of the multilayer growth on the ionic strength. For pure polycation/polyanion multilayers, it is well-known that the layer thickness or adsorbed mass increases with increasing ionic strength. This is explained by a shift in the polyelectrolyte charge compensation from intrinsic to extrinsic at higher ionic strengths, which is accompanied by thicker, more open, and mobile layers.[42,43] In contrast to this, for multilayers based on a polycation and a polyzwitterion, we showed recently that the layer mass dependence on the ionic strength behaves opposite: a decrease in layer mass is observed at higher ionic strength, which is predominantly attributed to the higher solubility of the zwitterion at higher ionic strengths, the so-called antipolyelectrolyte effect.[39,44] Figure 4 shows that the influence of this antipolyelectrolyte effect is also present for the PDADMAC/PSBMA/PSS trilayers. At the lowest ionic strength, the highest adsorbances are found, which is caused by the especially high adsorption of the polyzwitterion. With increasing ionic strength, the adsorption of PSBMA per coating step decreases. The decrease of PSBMA adsorption at higher ionic strengths also results in almost no significant PSBMA adsorption observed at 1.0 M. This means that at 1.0 M NaCl, we effectively observe the formation of almost pure PSS/PDADMAC bilayers. In parallel with the reduction of the PSBMA adsorption when coating at higher ionic strengths, the PDADMAC and PSS adsorption increases at higher ionic strength. This is a classical PEM behavior, caused by the shift to extrinsic charge compensation.[43] However, as the decrease in PSBMA adsorption is more pronounced, the net result is an overall decrease of the multilayer mass per trilayer at higher ionic strengths.

In addition to the changes of the layer masses adsorbed at different ionic strength, the adsorption kinetics also change as a function of the ionic strength. At 0.05 and 0.1 M, initially, an excess of PSBMA is adsorbed, which is then slowly rinsed away during the measurement. At 0.2 M NaCl a stable layer growth is observed, comparable to growth of classical PEMs.[42] Similar observations in dynamics during the coating of polycation/polyzwitterion multilayers at different ionic strengths were previously observed,[39] attributed to solubility changes and concentration dependence of the nature of the formed PDADMAC/PSBMA complexes.[45] We reason that similar changes in the solubility of the different complexes of the PDADMAC, PSBMA, and PSS can be attributed to the different growth dynamics observed here. Furthermore, at 0.2 M NaCl, the amount of polymer adsorbed per layer is similar for all three polyelectrolytes. Because of this even distribution between the three different polyelectrolytes at 0.2 M NaCl and the fact that this concentration shows the most stable layer growth, further experiments are performed with trilayers grown at 0.2 M NaCl.

The wettability of the multilayers coated from 0.2 M NaCl was investigated for different terminating layers by means of contact angle measurements. The contact angle measurements give insight into the hydrophilicity of the layers, which is especially important for water filtration applications. As expected, the results presented in Table 2, show a change of the layer hydrophilicity for differently terminating layers. The

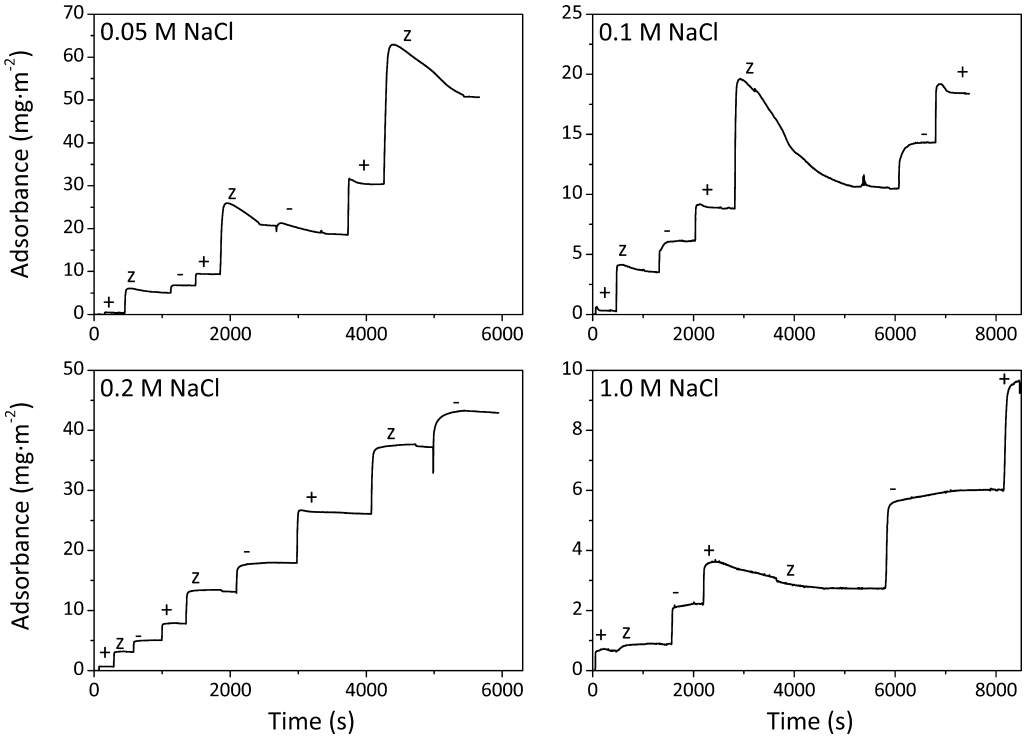

Figure 4. Typical reflectometry graphs showing the subsequent adsorption of PDADMAC (+), PSBMA (z), and PSS (−) from (top left) 0.05, (top right) 0.1, (bottom left) 0.2, and (bottom right) 1.0 M NaCl solutions. Note the different *y* axis scales for each graph.

Table 2. Trilayer Contact Angle Measurements on Silicon Wafers for Different Terminating Layers

layer	contact angle (deg)
$(PDADMAC/PSBMA/PSS)_1$-PDADMAC (+)	55.9 ± 11.4
$(PDADMAC/PSBMA/PSS)_1$-PDADMAC/PSBMA (z)	72.5 ± 7.1
$(PDADMAC/PSBMA/PSS)_2$ (−)	32.1 ± 4.0

high contact angle obtained for PSBMA-terminated layers is a result of the antipolyelectrolyte effect: in pure water, the zwitterionic polymer has a hydrophobic nature due to the high interchain interactions of the zwitterionic charges.[44] Both the PDADMAC- and PSS-terminated layers are more hydrophilic as compared to the zwitterionic terminated layers. When comparing only the two polyelectrolytes, the lowest contact angle is observed for PSS-terminated layers, which is comparable to what was found for pure PDADMAC/PSS bilayers.[46]

3.2. Polymeric Hollow Fiber Membrane Modification.

Polymeric hollow fiber membranes (HFS membranes from Pentair X-Flow) were coated with the polyelectrolyte trilayers from solutions containing 0.2 M NaCl. After each coating step, a membrane sample was taken for permeability and zeta-potential measurements. The results in Figure 5 show the successful trilayer growth on the membrane. With the addition of more polyelectrolyte trilayers on the membrane, the permeability significantly decreases, especially after the first layers. After each PDADMAC and PSBMA addition, the permeability decreases, which is a clear indication of polymer adsorption. However, with each PSS addition, the permeability increases again. Our reflectometry results show that this increase in permeability cannot be caused by material removal

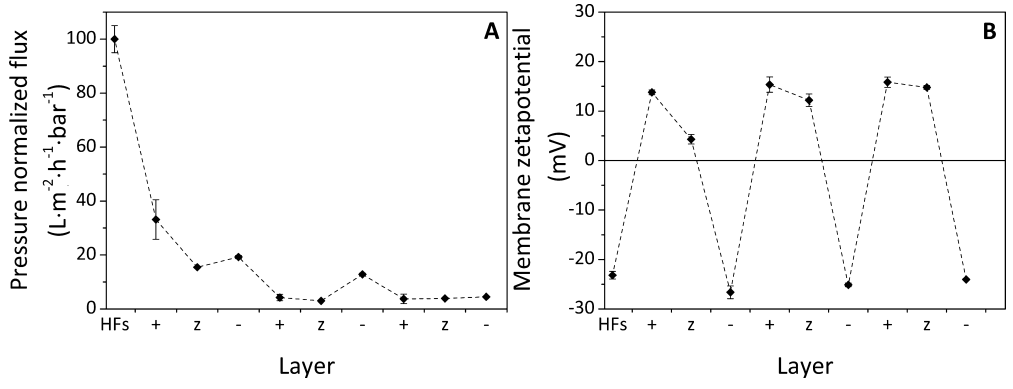

Figure 5. HFS membrane modification with trilayers of PDADMAC (+), PSBMA (z), and PSS (−) from 0.2 M NaCl: (A) HFS-modified membrane permeability ($l \cdot m^{-2} \cdot h^{-1} \cdot bar^{-1}$) after each additional layer. (B) Membrane zetapotential (mV) after each coating step, measured in 5 mM KCl at pH 5.8. For all points, the error bars indicate the standard deviation.

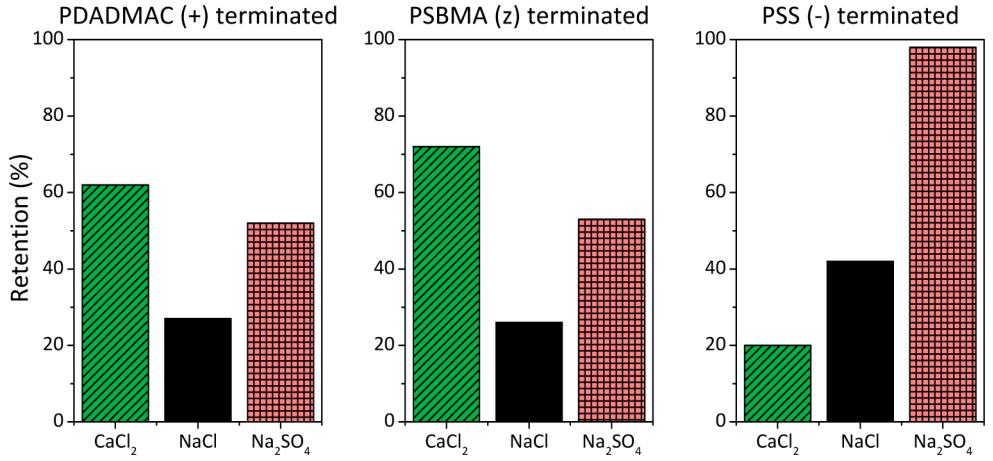

Figure 6. Different ion retentions of the HFS membranes coated with $(PDADMAC/PSBMA/PSS)_2/PDADMAC$ (+), $(PDADMAC/PSBMA/PSS)_2/PDADMAC/PSBMA$ (z), and $(PDADMAC/PSBMA/PSS)_3$ (−). Ion feed concentration is 5 mM. The filtration is performed under cross-flow at turbulent conditions ($R_e \approx 3500$) and a trans-membrane pressure of 1.75 bar.

during the PSS step, because no layer loss is observed while coating from 0.2 M NaCl (Figure 4). This means that a PSS-terminated layer is itself more permeable to water, even though more polymer in total is adsorbed on the membrane. Such increases in permeability after an additional coating can be attributed to a change in water affinity of the different terminating layers.[47,48] Our contact angle measurements of the multilayers indeed show the lowest contact angle for the PSS-terminated layer, supporting that the increase in the membrane permeability is caused by the higher hydrophilicity of the PSS-terminated layers.

Next to an understanding of the membrane permeability, the membrane zeta-potential measurements after each additional layer provide insight into the formation of the trilayers on the fiber. As shown in Figure 5B, a complete charge reversal of the negative membrane surface occurs when a PDADMAC layer is applied. The subsequent coating of the essentially neutral PSBMA results in a slightly lower yet still positive membrane. The absence of charge reversal is explained by the charge neutrality of the polyzwitterion and was also observed for membranes coated with PDADMAC/PSBMA bilayers.[39] Charge reversal is again obtained when the PSBMA-terminated layer is coated with PSS, resulting in a negatively charged membrane. This charge reversal after the PSS addition also confirms the adsorption of PSS on the membrane. For each additional trilayer, the same behavior of charge reversal by the addition of only PDADMAC and PSS is observed. These results on the hollow fiber membrane, which are in good agreement with the experiments on model surfaces, show the possibility of incorporating a zwitterionic polymer into a polyanion- and polycation-based PEM, both on model surfaces and on porous membranes.

3.3. Polymeric Hollow Fiber Membrane Performance. The performance of our membranes coated with different layers is determined by their ability to retain different solutes. To study this, membranes were taken that were coated with 7, 8, or 9 monolayers, and which were thus terminated with either PDADMAC (+), PSBMA (z), or PSS(−). This provides insight into the effect of the terminating layer. NF membranes are typically characterized by their ability to retain different salts.[49] Several models have been developed to describe the rejections of ions, taking size, charge, valence, and dielectric exclusion into account.[49−51] A characteristic dependence on the ion valence is typical for Donnan exclusion, while the dielectric exclusion accounts for the interactions of ions with polarized interfaces between media of different dielectric constants. As a result of dielectric exclusion, both anions and cations are excluded from the membranes (nano)pores. In the case of charged NF membranes, Donnan exclusion was shown to be the main parameter determining the rejection.[42,52] In previous work, we showed that this was indeed true for membranes coated with $(PDADAMC/PSS)_6$−PDADMAC and $(PDADMAC/PSS)_7$.[42] However, recent work of Bruening and co-workers showed that for charged LbL modified membranes, size exclusions can also be the main mechanism.[53] It was further shown that when Donnan effects and size exclusion do not suffice to describe the retention behavior, the dielectric exclusion needs to be taken into account.[50,51] To our knowledge, the effect of the presence of zwitterionic moieties in multilayers on the rejection mechanism for nanofiltration purposes has not been studied yet.

In Figure 6, the retention of $CaCl_2$, NaCl, and Na_2SO_4 for the three different membranes is shown. No permeability changes were observed during the filtration of the electrolyte solution compared to the clean water permeabilities (3.9, 3.7, and 4.5 $l \cdot m^{-2} \cdot h^{-1} \cdot bar^{-1}$ for the membranes coated with 7 (+), 8 (z), and 9(−) layers, respectively). The rejection results of the different salts by the membranes provide an insight of the major retention mechanism. The PSS-terminated membrane indeed shows a typical Donnan behavior. Due to an increased Donnan exclusion of the bivalent sulfate anion by the negative membrane, almost complete retention (98%) for Na_2SO_4 is observed. The bivalent calcium cation, on the other hand, is excluded the least by the negative membrane, resulting in only 20% retention for $CaCl_2$. In line with these results, the NaCl retention is found between that of Na_2SO_4 and $CaCl_2$. In contrast to the PSS-terminated membrane, neither the PDADMAC- nor the PSBMA-terminated membranes show clear Donnan behavior. For these membranes, which are positively charged, the retention of both Na_2SO_4 and $CaCl_2$ is higher compared to that of NaCl. If Donnan exclusion were prevalent, the expected order of salt retention would be $CaCl_2$ > NaCl > Na_2SO_4. This indicates that size and dielectric exclusion of Ca^{2+} and SO_4^{2-} dominate the retention. The difference between the salt retention of our differently terminated trilayers is remarkable and was not observed for

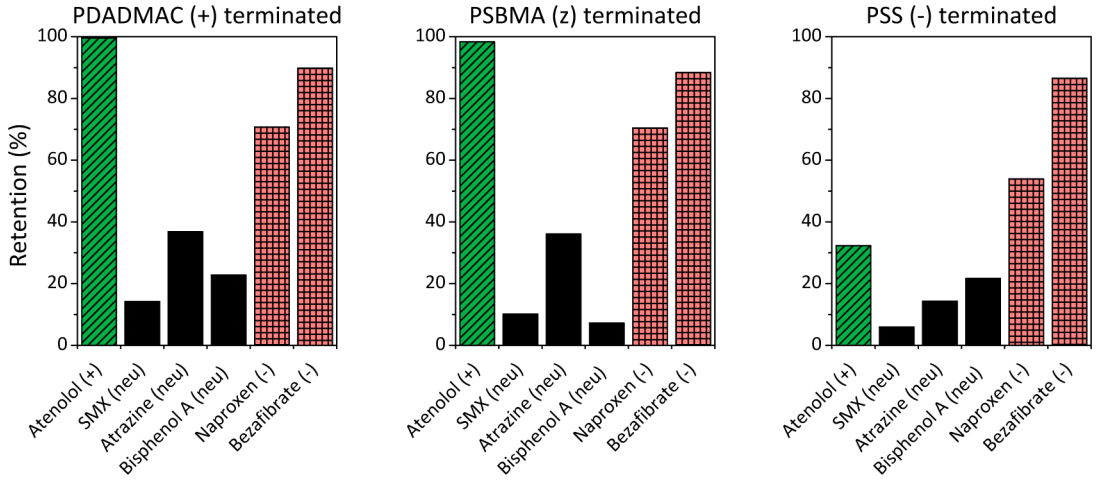

Figure 7. Retention of different micropollutants at pH 5.8 by HFS membranes coated with $(PDADMAC/PSBMA/PSS)_2/PDADMAC$ (+), $(PDADMAC/PSBMA/PSS)_2/PDADMAC/PSBMA$ (z), and $(PDADMAC/PSBMA/PSS)_3$ (−). Filtration experiments were performed under turbulent conditions ($R_e \approx 3{,}500$) and at a trans-membrane pressure of 1.75 bar. Results are color coded based on the micropollutant charge: (green) positive, (black) neutral, and (red) negative.

PDADMAC/PSS bilayers. Therefore, any contributions from dielectric exclusion can only be attributed to the presence of the zwitterion PSBMA within the multilayer.

In addition to the retention behavior for different salts, the retention for a mixture of six micropollutants was also measured for membranes coated with 7 (+), 8 (z), or 9 (−) layers. The selected micropollutants are shown in Figure 3, and some important properties are listed in Table 1. During the selection, care was taken that positive, neutral, and negative molecules were included. Furthermore, a wide range of hydrophilicity was taken. The octanol/water coefficients (log P) of the different micropollutants range from 0.49 (most hydrophilic) to 4.04 (most hydrophobic). The filtration experiments were conducted under circumstances similar to those for the ion rejection measurements. As with the electrolyte solutions, no difference in permeability compared to the clean water permeability was observed during the measurement. Figure 7 shows the results, which have been color coded based on the micropollutant charge: green for positive micropollutants, black for neutral micropollutants, and red for negative micropollutants.

For all three membranes, the micropollutant rejection mechanisms are comparable to those observed for the salt rejections. In the case of the PSS-terminated membrane, evidence of Donnan exclusion is found. Both naproxen and bezafibrate are negatively charged and show a high retention. This high retention is attributed to the charge repulsion of the negative membrane, and is comparable to the high SO_4^{2-} retention. A significantly lower retention is observed for the positively charged atenolol by the negative membrane, comparable to Ca^{2+} retention. Due to the opposite charges of the atenolol (positive) and the PSS-terminated membrane (negative) little charge repulsion exists, resulting in a lower retention compared to that of the negative micropollutants. The lack of charges of the three neutral micropollutants results in the lowest retention for these molecules, as no electric repulsion exists, and the rejection is primarily based on size exclusion.

In contrast to the PSS-terminated layer, the PDADMAC- and PSBMA-terminated layers show high retention of all charged micropollutants. The three uncharged micropollutants have a significantly lower retention compared to that of the charged micropollutants. This is similar to that observed for the PSS-terminated membrane, which also shows lower retention for uncharged species. Even though Donnan exclusion is not prevalent in the PDADMAC- and PSBMA-terminated membranes, the results from the micropollutant filtration show that the retention cannot be (solely) based on size exclusion. For these membranes, no trend with respect of the molecular weight of the micropollutant is found, for example, for the PSBMA-terminated membrane, 70.4% of naproxen (230.26 $g \cdot mol^{-1}$) is retained, whereas only 7.2% of bisphenol A (228.29 $g \cdot mol^{-1}$) is retained, even though these molecules have similar dimensions.[6] This means that, by the incorporation of the zwitterionic layer, the dielectric exclusion determines the solute rejection. As a result, these membranes have a high retention for all charged solutes. This is a significant advantage in water treatment processes because more contaminants can be rejected in a single step as compared to membranes that only show Donnan exclusion.

4. CONCLUSION

Current challenges in drinking water contamination require the development of much more sophisticated, specific, and straightforward purification techniques designed to remove low molecular weight contaminants based on direct nanofiltration (NF) with hollow fibers membranes. Such hollow fiber membranes should have a separation layer that rejects a multitude of contaminants. In this work, we present a new hollow fiber NF membrane based on PDADMAC (+), PSBMA (z), and PSS (−) trilayers coated from aqueous solutions onto a membrane support using the simple LbL coating approach. On model surfaces, the ionic strength of the coating solutions is found to be a key parameter to control the stability and growth of these layers, with the most stable layer growth obtained at 0.2 M NaCl. Under these conditions, the trilayers can also be successfully coated on charged porous membranes. The properties of the formed NF membranes depend strongly on the terminating layer. Due to the higher hydrophilicity of a PSS-terminated layer, membranes with a final PSS coating have a relatively higher water permeability compared to membranes that have a PDADMAC- or PSBMA-terminated layer. The

retention of different solutes in water and the underlying mechanism change with the terminating layer. For all membranes, the rejection of uncharged micropollutants is relatively low due to the lack of Donnan or dielectric exclusion. For PSS-terminated layers, clear evidence of Donnan exclusion is found, resulting in a membrane with Na_2SO_4 rejection of 98% at a permeability of 4.5 $l \cdot m^{-2} \cdot h^{-1} \cdot bar^{-1}$. This Donnan exclusion is also manifested in the rejection of micropollutants, where only high rejection of negatively charged molecules is observed. For membranes with either PDADMAC- or PSBMA-terminated layers, the difference in the rejection of various ion pairs cannot be described by Donnan exclusion, and it is concluded that dielectric exclusion is the dominating rejection mechanism. As a result of this, membranes, terminated with either PDADMAC or PSBMA have a high retention for both positively and negatively charged micropollutants. This behavior is not seen for classical PDADMAC and PSS PEMs, and is therefore attributed to the incorporation of the polyzwitterion in the multilayer. Because these zwitterionic NF membranes are able to retain a wider variety of micropollutants, they are better suited for the removal of emerging contaminants from polluted water.

This work shows the value of the combination of investigating the growth of multilayers on model surfaces and the performance of LbL-coated membranes. The complementary results, such as multilayer growth, contact angle, and membrane zeta-potential and permeability, help in understanding the nature and behavior of the multilayers. This combination is especially powerful when macromolecules with particular functionalities (such as polyzwitterions) are introduced into the multilayer system for the specific design of NF membranes.

AUTHOR INFORMATION

Corresponding Author

*E-mail: w.m.devos@utwente.nl.

Notes

The authors declare no competing financial interest.

ACKNOWLEDGMENTS

The authors would like to thank Pentair X-Flow for the financial support on this work and Dr. Jens Potreck for the in-depth discussions on the results.

REFERENCES

(1) van der Aa, N. G. F. M.; Dijkman, E.; Bijlsma, L.; Emke, E.; van de Ven, B. M.; Nuijs, A. L. N.; de Voogt, P. *Drugs of Abuse and Tranquilizers in Dutch Surface Waters, Drinking Water, and Wastewater: Results of Screening Monitoring in 2009*; RIVM Report 703719064; National Institute for Public Health and the Environment: Bilthoven, The Netherlands, 2010.

(2) Schriks, M.; Heringa, M. B.; van der Kooi, M. M. E.; de Voogt, P.; van Wezel, A. P. Toxicological Relevance of Emerging Contaminants for Drinking Water Quality. *Water Res.* **2010**, *44* (2), 461−476.

(3) de Voogt, P.; Janex-Habibi, M. L.; Sacher, F.; Puijker, L.; Mons, M. Development of a Common Priority List of Pharmaceuticals Relevant for the Water Cycle. *Water Sci. Technol.* **2009**, *59* (1), 39−46.

(4) *De Kwaliteit Van Het Maaswater in 2012*; RIWA, Vereniging van Rivierwaterbedrijven: Nieuwegein, The Netherlands, 2013.

(5) Priority Substances and Certain Other Pollutants According to Annex II of Directive 2008/105/EC, *EU Water Framework Directive*; European Parliament and Council, 2008.

(6) Yangali-Quintanilla, V.; Maeng, S. K.; Fujioka, T.; Kennedy, M.; Amy, G. Proposing Nanofiltration as Acceptable Barrier for Organic Contaminants in Water Reuse. *J. Membr. Sci.* **2010**, *362* (1−2), 334−345.

(7) Bellona, C.; Heil, D.; Yu, C.; Fu, P.; Drewes, J. E. The Pros and Cons of Using Nanofiltration in Lieu of Reverse Osmosis for Indirect Potable Reuse Applications. *Sep. Purif. Technol.* **2012**, *85*, 69−76.

(8) Hajibabania, S.; Verliefde, A.; McDonald, J. A.; Khan, S. J.; Le-Clech, P. Fate of Trace Organic Compounds During Treatment by Nanofiltration. *J. Membr. Sci.* **2011**, *373* (1−2), 130−139.

(9) Plakas, K. V.; Karabelas, A. J. Removal of Pesticides from Water by NF and RO Membranes—A Review. *Desalination* **2012**, *287*, 255−265.

(10) Nghiem, L. D.; Schäfer, A. I.; Elimelech, M. Pharmaceutical Retention Mechanisms by Nanofiltration Membranes. *Environ. Sci. Technol.* **2005**, *39* (19), 7698−7705.

(11) Yoon, Y.; Westerhoff, P.; Snyder, S. A.; Wert, E. C. Nanofiltration and Ultrafiltration of Endocrine Disrupting Compounds, Pharmaceuticals and Personal Care Products. *J. Membr. Sci.* **2006**, *270* (1−2), 88−100.

(12) Klüpfel, A. M.; Frimmel, F. H. Nanofiltration of River Water—Fouling, Cleaning, and Micropollutant Rejection. *Desalination* **2010**, *250* (3), 1005−1007.

(13) Nghiem, L. D.; Coleman, P. J.; Espendiller, C. Mechanisms Underlying the Effects of Membrane Fouling on the Nanofiltration of Trace Organic Contaminants. *Desalination* **2010**, *250* (2), 682−687.

(14) Kiso, Y.; Muroshige, K.; Oguchi, T.; Yamada, T.; Hhirose, M.; Ohara, T.; Shintani, T. Effect of Molecular Shape on Rejection of Uncharged Organic Compounds by Nanofiltration Membranes and on Calculated Pore Radii. *J. Membr. Sci.* **2010**, *358* (1−2), 101−113.

(15) Yangali-Quintanilla, V.; Sadmani, A.; McConville, M.; Kennedy, M.; Amy, G. Rejection of Pharmaceutically Active Compounds and Endocrine Disrupting Compounds by Clean and Fouled Nanofiltration Membranes. *Water Res.* **2009**, *43* (9), 2349−2362.

(16) Hilal, N.; Al-Zoubi, H.; Darwish, N. A.; Mohamma, A. W.; Abu Arabi, M. A Comprehensive Review of Nanofiltration Membranes: Treatment, Pretreatment, Modelling, and Atomic Force Microscopy. *Desalination* **2004**, *170* (3), 281−308.

(17) Al-Amoudi, A.; Lovitt, R. W. Fouling Strategies and the Cleaning System of NF Membranes and Factors Affecting Cleaning Efficiency. *J. Membr. Sci.* **2007**, *303* (1−2), 4−28.

(18) Vince, F.; Aoustin, E.; Bréant, P.; Marechal, F. LCA Tool for the Environmental Evaluation of Potable Water Production. *Desalination* **2008**, *220* (1−3), 37−56.

(19) Veríssimo, S.; Peinemann, K. V.; Bordado, J. New Composite Hollow Fiber Membrane for Nanofiltration. *Desalination* **2005**, *184* (1−3), 1−11.

(20) Kiso, Y.; Mizuno, A.; Othman, R. A. A. b.; Jung, Y.-J.; Kumano, A.; Ariji, A. Rejection Properties of Pesticides with a Hollow Fiber NF Membrane (HNF-1). *Desalination* **2002**, *143* (2), 147−157.

(21) Simon, A.; Nghiem, L. D.; Le-Clech, P.; Khan, S. J.; Drewes, J. E. Effects of Membrane Degradation on the Removal of Pharmaceutically Active Compounds (PhACs) by NF/RO Filtration Processes. *J. Membr. Sci.* **2009**, *340* (1−2), 16−25.

(22) He, T.; Frank, M.; Mulder, M. H. V.; Wessling, M. Preparation and Characterization of Nanofiltration Membranes by Coating Polyethersulfone Hollow Fibers with Sulfonated Poly(ether ether ketone) (SPEEK). *J. Membr. Sci.* **2008**, *307* (1), 62−72.

(23) Jung, Y. J.; Kiso, Y.; Adawih, binti; Othman, R. A.; Ikeda, A.; Nishimura, K.; Min, K. S.; Kumano, A.; Ariji, A. Rejection Properties of Aromatic Pesticides with a Hollow-Fiber NF Membrane. *Desalination* **2005**, *180* (1−3), 63−71.

(24) Song, J.; Li, X.-M.; Figoli, A.; Huang, H.; Pan, C.; He, T.; Jiang, B. Composite Hollow Fiber Nanofiltration Membranes for Recovery of Glyphosate from Saline Wastewater. *Water Res.* **2013**, *47* (6), 2065−2074.

(25) Toutianoush, A.; Jin, W.; Deligöz, H.; Tieke, B. Polyelectrolyte Multilayer Membranes for Desalination of Aqueous Salt Solutions and Seawater under Reverse Osmosis Conditions. *Appl. Surf. Sci.* **2005**, *246* (4), 437−443.

(26) Bruening, M. L.; Adusumilli, M. Polyelectrolyte Multilayer Films and Membrane Functionalization. *Mater. Matters* **2011**, *6* (3), 76−81.
(27) Joseph, N.; Ahmadiannamini, P.; Hoogenboom, R.; Vankelecom, I. F. J. Layer-by-Layer Preparation of Polyelectrolyte Multilayer Membranes for Separation. *Polym. Chem.* **2014**, *5* (6), 1817−1831.
(28) Decher, G. Fuzzy Nanoassemblies: Toward Layered Polymeric Multicomposites. *Science* **1997**, *277* (5330), 1232−1237.
(29) Setiawan, L.; Wang, R.; Li, K.; Fane, A. G. Fabrication and Characterization of Forward Osmosis Hollow Fiber Membranes with Antifouling NF-Like Selective Layer. *J. Membr. Sci.* **2012**, *394*−*395*, 80−88.
(30) Liu, C.; Fang, W.; Chou, S.; Shi, L.; Fane, A. G.; Wang, R. Fabrication of Layer-by-Layer Assembled FO Hollow Fiber Membranes and Their Performances Using Low Concentration Draw Solutions. *Desalination* **2013**, *308* (0), 147−153.
(31) Kharlampieva, E.; Izumrudov, V. A.; Sukhishvili, S. A. Electrostatic Layer-by-Layer Self-Assembly of Poly(carboxybetaine)s: Role of Zwitterions in Film Growth. *Macromolecules* **2007**, *40* (10), 3663−3668.
(32) Glinel, K.; Déjugnat, C.; Prevot, M.; Schöler, B.; Schönhoff, M.; Klitzing, R. v. Responsive Polyelectrolyte Multilayers. *Colloids Surf., A* **2007**, *303* (1−2), 3−13.
(33) Chapel, J. P.; Berret, J. F. Versatile Electrostatic Assembly of Nanoparticles and Polyelectrolytes: Coating, Clustering and Layer-by-Layer Processes. *Curr. Opin. Colloid Interface Sci.* **2012**, *17* (2), 97−105.
(34) Cooper, C. L.; Dubin, P. L.; Kayitmazer, A. B.; Turksen, S. Polyelectrolyte−Protein Complexes. *Curr. Opin. Colloid Interface Sci.* **2005**, *10* (1−2), 52−78.
(35) Kudaibergenov, S.; Jaeger, W.; Laschewsky, A. *Polymeric Betaines: Synthesis, Characterization, and Application*. Springer-Verlag: Berlin, Heidelberg, 2006; Vol. *201*, pp 157−224.
(36) Estephan, Z. G.; Schlenoff, P. S.; Schlenoff, J. B. Zwitteration as an Alternative to Pegylation. *Langmuir* **2011**, *27* (11), 6794−6800.
(37) Ji, Y.-L.; An, Q.-F.; Zhao, Q.; Sun, W.-D.; Lee, K.-R.; Chen, H.-L.; Gao, C.-J. Novel Composite Nanofiltration Membranes Containing Zwitterions with High Permeate Flux and Improved Anti-Fouling Performance. *J. Membr. Sci.* **2012**, *390*−*391* (0), 243−253.
(38) Kim, J.-H.; Park, P.-K.; Lee, C.-H.; Kwon, H.-H. Surface Modification of Nanofiltration Membranes to Improve the Removal of Organic Micro-Pollutants (EDCs and PhACs) in Drinking Water Treatment: Graft Polymerization and Cross-Linking Followed by Functional Group Substitution. *J. Membr. Sci.* **2008**, *321* (2), 190−198.
(39) de Grooth, J.; Dong, M.; de Vos, W. M.; Nijmeijer, K. Building Polyzwitterion-Based Multilayers for Responsive Membranes. *Langmuir* **2014**, *30* (18), 5152−61.
(40) Dijt, J. C.; Stuart, M. A. C.; Fleer, G. J. Reflectometry as a Tool for Adsorption Studies. *Adv. Colloid Interface Sci.* **1994**, *50*, 79−101.
(41) de Vos, W. M.; de Keizer, A.; Stuart, M. A. C.; Kleijn, J. M. Thin Polymer Films as Sacrificial Layers for Easier Cleaning. *Colloids Surf., A* **2010**, *358* (1−3), 6−12.
(42) de Grooth, J.; Oborny, R.; Potreck, J.; Nijmeijer, K.; de Vos, W. M. The Role of Ionic Strength and Odd-Even Effects on the Properties of Polyelectrolyte Multilayer Nanofiltration Membranes. *J. Membr. Sci.* **2014**, Submitted for publication.
(43) Schlenoff, J. B.; Ly, H.; Li, M. Charge and Mass Balance in Polyelectrolyte Multilayers. *J. Am. Chem. Soc.* **1998**, *120* (30), 7626−7634.
(44) Schultz, D. N.; Peiffer, D. G.; Agarwal, P. K.; Larabee, J.; Kaladas, J. J.; Soni, L.; Handwerker, B.; Garner, R. T. Phase Behaviour and Solution Properties of Sulphobetaine Polymers. *Polymer* **1986**, *27* (11), 1734−1742.
(45) Mary, P.; Bendejacq, D. D. Interactions between Sulfobetaine-Based Polyzwitterions and Polyelectrolytes. *J. Phys. Chem. B* **2008**, *112* (8), 2299−2310.
(46) Elzbieciak, M.; Kolasinska, M.; Warszynski, P. Characteristics of Polyelectrolyte Multilayers: The Effect of Polyion Charge on Thickness and Wetting Properties. *Colloids Surf., A* **2008**, *321* (1−3), 258−261.
(47) Wong, J. E.; Rehfeldt, F.; Hänni, P.; Tanaka, M.; Klitzing, R. v. Swelling Behavior of Polyelectrolyte Multilayers in Saturated Water Vapor. *Macromolecules* **2004**, *37* (19), 7285−7289.
(48) Su, B.; Wang, T.; Wang, Z.; Gao, X.; Gao, C. Preparation and Performance of Dynamic Layer-by-Layer PDADMAC/PSS Nanofiltration Membrane. *J. Membr. Sci.* **2012**, *423*−*424* (0), 324−331.
(49) Schafer, A. I., Fane, A. G., Waite, T. D., Eds.*Nanofiltration: Principles and Applications*; Elsevier Advanced Technology: New York, 2005.
(50) Szymczyk, A.; Fievet, P. Investigating Transport Properties of Nanofiltration Membranes by Means of a Steric, Electric, and Dielectric Exclusion Model. *J. Membr. Sci.* **2005**, *252* (1−2), 77−88.
(51) Yaroshchuk, A. E. Dielectric Exclusion of Ions from Membranes. *Adv. Colloid Interface Sci.* **2000**, *85* (2−3), 193−230.
(52) Peeters, J. M. M.; Boom, J. P.; Mulder, M. H. V.; Strathmann, H. Retention Measurements of Nanofiltration Membranes with Electrolyte Solutions. *J. Membr. Sci.* **1998**, *145* (2), 199−209.
(53) Cheng, C.; Yaroshchuk, A.; Bruening, M. L. Fundamentals of Selective Ion Transport through Multilayer Polyelectrolyte Membranes. *Langmuir* **2013**, *29* (6), 1885−1892.